ACADEMIC PRESS

Available online at www.sciencedirect.com

SCIENCE DIRECT®

VIROLOGY

Virology 312 (2003) 122–134

www.elsevier.com/locate/yviro

Rhesus monkey rhadinovirus (RRV): construction of a RRV-GFP recombinant virus and development of assays to assess viral replication

Scott M. DeWire,[a] Eric S. Money,[b] Stuart P. Krall,[b] and Blossom Damania[a,b,*]

[a] *Curriculum in Genetics and Molecular Biology, University of North Carolina at Chapel Hill, Chapel Hill, NC 27599, USA*

[b] *Department of Microbiology & Immunology and Lineberger Comprehensive Cancer Center, University of North Carolina at Chapel Hill, Chapel Hill, NC 27599, USA*

Received 14 November 2002; returned to author for revision 9 January 2003; accepted 21 February 2003

Abstract

Rhesus monkey rhadinovirus (RRV) is a γ-2-herpesvirus that is closely related to Kaposi's sarcoma-associated herpesvirus (KSHV/HHV-8). Lack of an efficient culture system to grow high titers of virus, and the lack of an in vivo animal model system, has hampered the study of KSHV replication and pathogenesis. RRV is capable of replicating to high titers on fibroblasts, thus facilitating the construction of recombinant rhadinoviruses. In addition, the ability to experimentally infect naïve rhesus macaques with RRV makes it an excellent model system to study γ-herpesvirus replication. Our study describes, for the first time, the construction of a GFP-expressing RRV recombinant virus using a traditional homologous recombination strategy. We have also developed two new methods for determining viral titers of RRV including a traditional viral plaque assay and a quantitative real-time PCR assay. We have compared the replication of wild-type RRV with that of the RRV-GFP recombinant virus in one-step growth curves. We have also measured the sensitivity of RRV to a small panel of antiviral drugs. The development of both the recombination strategy and the viral quantitation assays for RRV will lay the foundation for future studies to evaluate the contribution of individual genes to viral replication both in vitro and in vivo.

Keywords: Rhesus monkey rhadinovirus; Real-time PCR; Plaque assay; Recombinant rhadinovirus

Introduction

In 1994, Chang and Moore identified Kaposi's sarcoma-associated herpesvirus (KSHV/HHV-8) in Kaposi's sarcoma biopsies by representative differential analysis (Chang et al., 1994). KSHV has since been implicated as the causative agent for Kaposi's sarcoma (Ganem, 1998; Kedes et al., 1996; Miller et al., 1996; Moore and Chang, 1995), primary effusion lymphomas (Cesarman et al., 1995; Chang et al., 1994), and multicentric Castleman's disease (MCD) (Gessain et al., 1996; Soulier et al., 1995). Understanding the replication and pathogenesis of this virus has proven to be difficult due to the lack of an efficient lytic system to grow high titers of virus. KSHV studies involving the lytic cycle must be carried out in latently infected B cell lines using an artificial reactivation with phorbol esters, such as *n*-butyrate or tetradecanoyl phorbol acetate (TPA) (Miller et al., 1997; Renne et al., 1996). This scenario is unfavorable for a number of reasons including the fact that there is a very high background of latency, as only 25–30% of cells reactivate, and the potential for TPA-related artifacts (Chan et al., 1998; Renne et al., 1996). Alternatively a number of endothelial cell based systems have been established by several laboratories (Dezube et al., 2002; Lagunoff et al., 2002; Sakurada et al., 2001), but an inability to serially transmit the virus over an extended passage of time coupled with a high background of latency in these cell lines is a limiting factor for studying the KSHV lytic cycle. As a result, studies of either the KSHV viral replicative cycle or the consequences of infection on the host cell are very difficult to interpret. Other animal model systems have been

* Corresponding author. Lineberger Comprehensive Cancer Center, CB #7295 University of North Carolina, Chapel Hill, NC 27599. Fax: +1-919-966-9673.

E-mail address: damania@med.unc.edu (B. Damania).

0042-6822/03/$ – see front matter © 2003 Elsevier Science (USA). All rights reserved.
doi:10.1016/S0042-6822(03)00195-8

developed to assist in the understanding of γ-herpesvirus replication. Murine herpesvirus 68 (MHV-68) reviewed in Simas and Efstathiou (1998) and Herpesvirus saimiri (HVS) reviewed in Jung et al. (1999) are two such model viruses that have lytic cell-culture systems available.

At the New England Regional Primate Research Center (NERPRC), Desrosiers et al. (1997) discovered a novel γ-herpesvirus of rhesus monkeys (*Macacca mulatta*). The genomes of two isolates of this new virus, called rhesus monkey rhadinovirus (RRV) or RVMac2, were fully sequenced by the NERPRC and the Oregon Regional Primate Research Center (Alexander et al., 1999; Searles et al., 1999) to reveal that RRV is very closely related to KSHV. The NERPRC RRV strain has been designated H29-95. In addition, the concurrent finding of a cell line that supports lytic replication of RRV was an attribute that made RRV an attractive model to study KSHV. Since the sequencing of RRV, several primate rhadinoviruses with more similarity to KSHV have been discovered (Bosch et al., 1999; Rose et al., 1997; Schultz et al., 2000; Strand et al., 2000). However, due to complications with either virus isolation or identifying permissive cell culture systems, these viruses may not be tractable as model systems. Thus far, the RRV model has been used to study the viral interleukin-6 homologue (Kaleeba et al., 1999) and the R1 signaling protein (Damania et al., 1999, 2000). Further, the Rta/Orf50 immediate early transactivator, the bZIP homolog, also known as R8 or replication-associated protein (RAP), and the R8.1 glycoprotein have been identified and partially characterized independently by two groups of investigators (DeWire et al., 2002; Lin et al., 2002). We have also recently reported the kinetics of gene expression with regard to immediate-early, early, and late genes in RRV lytic infection (DeWire et al., 2002).

Here we describe the construction of a RRV-GFP recombinant virus and the development of two new viral quantitation assays for determining RRV titers. We compare the replication kinetics of wild-type RRV and the RRV-GFP recombinant virus by these two different techniques. One assay is a traditional plaque assay based on rhesus fibroblasts (RhFs), and the other is a quantitative real-time PCR assay. We demonstrate the usefulness of these assays by performing one-step growth curves for RRV and a GFP-expressing RRV recombinant virus and then test viral replication in the presence of several herpesviral-inhibitory compounds. With the increasing emergence of RRV as a model system for KSHV, we feel these assays will be valuable for assessing the replicative abilities of RRV as well as recombinant viruses derived from RRV, in reverse genetic studies.

Results

Traditionally, recombinant herpesviruses have been constructed by homologous recombination (Cann, 1999; Roizman and Jenkins, 1985). To determine a viral gene's contribution to replication and in vivo pathogenesis, one common strategy is to make recombinant viruses targeting a particular gene. To detect any replication defect in the recombinant virus, sensitive assays to determine viral titer in experimental samples are needed. In the work presented here, we have created, for the first time, a recombinant RRV that expresses the GFP gene and have assessed its replication in two different quantitative assays.

Construction of a RRV-GFP recombinant virus expressing green fluorescent protein (GFP)

We set forth to make a recombinant RRV that expresses GFP to use as a marker of infection in our quantitative assays, and also as a highly valuable tool for studying RRV pathogenesis in vivo in future studies. In order not to disrupt any RRV genes or their promoters, the GFP gene was introduced into a genomic location where two open reading frames (ORFs) terminate adjacent to each other (Fig. 1). We chose the region between ORFs 18 and 19, since the identical location has been disrupted in KSHV for the introduction of bacterial artificial chromosome sequences without any consequence to viral replication (Zhou et al., 2002). A GFP expression cassette driven by the cytomegalovirus immediate-early promoter was introduced using a traditional homologous recombination approach by cotransfection with RRV virion DNA into rhesus fibroblasts. A single plaque of GFP-expressing virus (Fig. 2) was purified four times by using limiting dilution, and a final purification by flow cytometry was performed. Purity and integrity of the virus was confirmed by different methods.

To verify that the insertion of exogenous sequences occurred only at the desired location, we performed Southern hybridization analysis (Figs. 3A, B, and C). The strategy we used to perform the Southern blots is depicted in Fig. 3A. Virion DNA from wt RRV and the RRV-GFP recombinant virus was isolated and restriction digested with *Sac*I. The DNA fragments were electrophoresed on an agarose gel and the gel was transferred to nitrocellulose. A Southern blot was performed using two different probes. Probe A was complementary to a region in ORF 18 and should hybridize to a 1876-bp fragment in wt RRV digested with *Sac*I and to a 3532-bp fragment in RRV-GFP virion DNA digested with *Sac*I. As can be seen in Fig. 3B, each of the wt RRV and RRV-GFP recombinant viruses gave us fragments of the expected size. Probe B was complementary to the GFP gene and when used in a Southern blot, we expected it to hybridize to the 3532-bp fragment of the *Sac*I-digested RRV-GFP DNA. Since the GFP gene is not present in wt RRV, we did not expect Probe B to hybridize to wt RRV DNA. Fig. 3C depicts the Southern blot performed on the samples using Probe B and shows that the GFP cassette was inserted into the RRV-GFP recombinant virus in the correct site and as expected, was absent in WT RRV DNA.

To further confirm our results, we also performed PCR

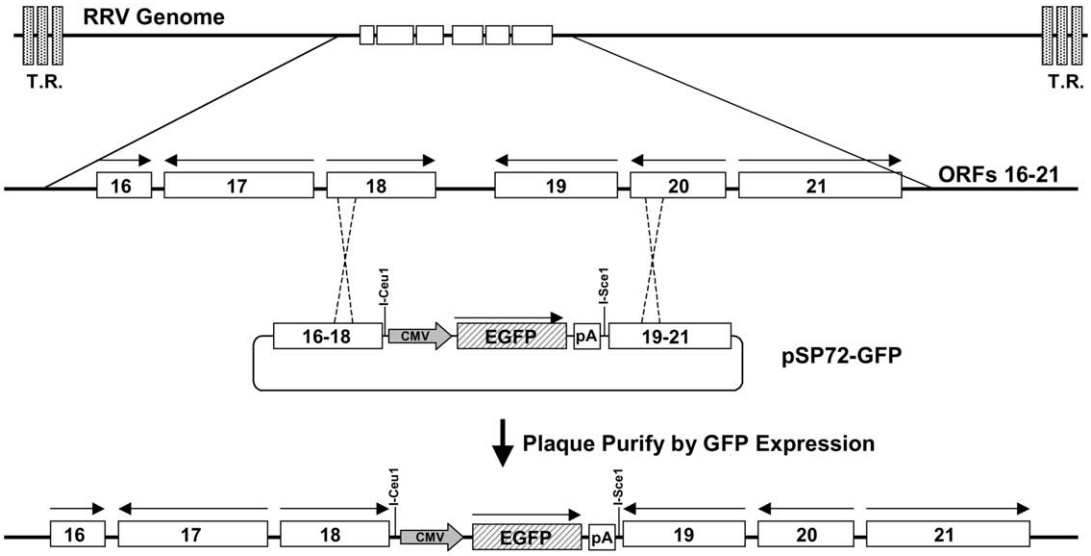

Fig. 1. A schematic representation of the construction of RRV-GFP. The region of the RRV genome between ORFs 18 and 19 was targeted for the introduction of a GFP expression cassette under the CMV promoter. This cassette was cloned into a plasmid in between the coding sequences for ORFs 16–18 and ORFs 19–21. The plasmid was then cotransfected into rhesus fibroblasts along with virion DNA, and a single GFP-expressing virus was purified.

amplification using primers flanking the ORF 18/19 junction (Fig. 3D). With the wt RRV virion DNA we were able to PCR-amplify the expected fragment of 150 bp using these primers, and with the RRV-GFP recombinant virion DNA, we PCR-amplified the expected fragment of 1800 bp using the same primers (Fig. 3D). We also performed DNA sequencing of these fragments and reconfirmed the integrity of these PCR-amplified fragments (data not shown).

Finally, to ensure that gene expression from the flanking ORFs 18 and 19 were not interrupted by the insertion of the GFP cassette into the RRV-GFP recombinant virus, we performed RT-PCR analysis on cells infected with both wt RRV and RRV-GFP recombinant viruses. Cells were infected with the respective viruses and poly(A) mRNA was isolated 72 h postinfection. RT-PCR was performed using primer sets that amplified ORF 18 and 19 transcripts, respectively. As can be seen in Fig. 3E, RT-PCR analysis of ORF 18 and 19 gene transcription in both parental WT RRV virus (lane 1) and recombinant RRV-GFP virus (lane 3) demonstrated that these flanking ORFs were transcribed to similar levels. Lanes 2 and 4 represent samples in which no reverse transcriptase was added to the RT-PCR reaction. As further confirmation that the RRV-GFP virus was not defective, plaques produced by the RRV-GFP virus were approximately the same size and grew with the same kinetics as the wild-type RRV H26-95 parent virus (Fig. 2).

The RRV plaque assay

Traditionally, the plaque assay has been the best means of quantifying viral loads. Plaque assays have been previously described for a number of herpesviruses (Garabedian and Scott, 1967; Gerna and Chambers, 1976; Wentworth and French, 1969, 1970; Yazaki et al., 1966). However, the agarose overlay based approach for plaque assays, which is widely used for many α-herpesviruses, was not tractable to the RRV lytic system. Here we report the development of a plaque assay for RRV based on a methyl-cellulose containing overlay. We attempted to assess RRV replication in a number of common cell types including 293-HEK, Vero, human embryonic lung, RhFs, and normal human fibroblasts. None of these cell types except for the rhesus fibroblasts were capable of supporting RRV replication and hence we designed our plaque assay using this cell line. Confluent monolayers of RhFs in 12-well dishes were infected with serially diluted RRV-H26-95 from a viral stock. After a viral adsorption incubation, wells were overlaid with a methyl-cellulose-containing media and then incubated at 37°C for 8 days, allowing plaques to form. A variety of overlay medias containing low-melt agarose from 0.6 to 1.2% and methyl-cellulose from 0.3 to 1.2% were attempted and it was found that the best media for efficient plaquing and cellular survival was 0.75% methyl-cellulose. After 7 days of incubation, overlay media was removed and cells were fixed and stained with crystal violet. A typical plaque assay dish is shown in Fig. 2B (panel A) and a typical RRV plaque is shown in Fig. 2D.

Use of RRV-GFP to determine plaquing efficiency

Next, we determined if every virus that infects cells on the plaque assay monolayer actually forms a plaque. The RRV system is said to be a completely lytic system, and using this virus and the plaquing technique we could confirm this assumption. To answer this question, we used the recombinant GFP-expressing virus, RRV-GFP (Figs. 1 and

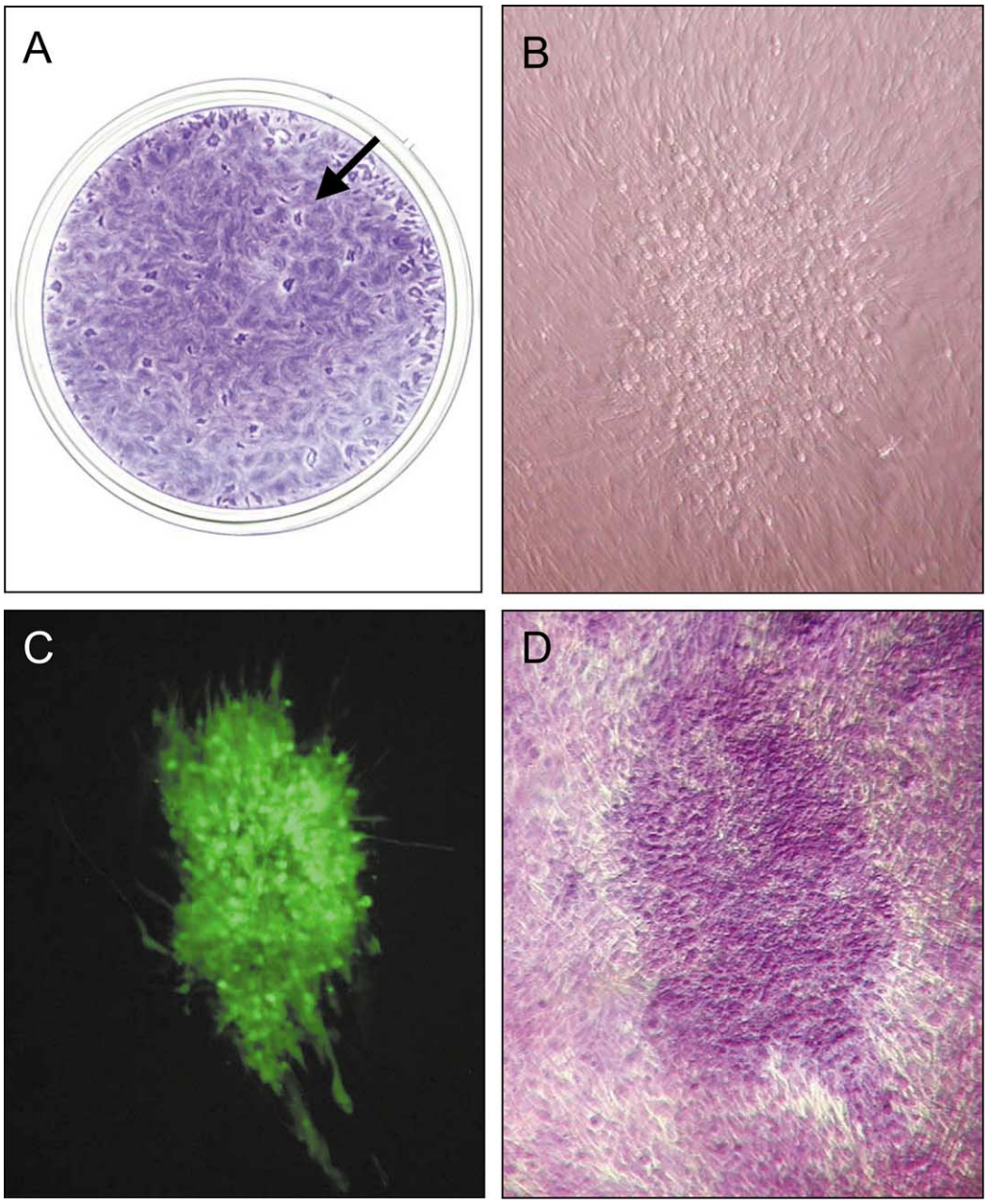

Fig. 2. Photographs of typical RRV/RRV-GFP Plaques. (A) A picture of a crystal violet preparation of a 35-mm dish from an RRV plaque assay showing the relative size of the plaques. (B) A single RRV-GFP plaque shown under phase contrast microscopy at ×100 magnification while still under overlay media. (C) The same plaque as in (B) shown with GFP excitation. (D) The same plaque as in (B) and (C) in final crystal violet preparation.

2), and traced the fate of GFP-expressing cells. We performed the aforementioned plaque assay with the recombinant virus and observed GFP expression through the microscope. At 2 days postinfection, we counted the number of GFP-positive cells in each well of the plaque assay dishes. Following the 7 day incubation, we counted the plaque numbers first by GFP expression and then by crystal violet staining. We concluded that every cell that expresses GFP at 2 *d.p.i.* contributes to a plaque at day 8, thus confirming the 100% lytic nature of RRV in rhesus fibroblasts. Fig. 2B shows an example of a GFP-positive plaque at 7 days postinfection in phase contrast (panel B), GFP fluorescence (panel C), and final crystal violet preparation (panel D).

The RRV real-time qPCR assay

Real-time PCR, first described by Heid et al. (1996), is a highly sensitive and accurate method for quantifying copy number of a target DNA sequence. As a result of the speed and reliability of these types of assays, quantitative real-time PCR assays have been previously established for a number of herpesviruses for use in both research and clin-

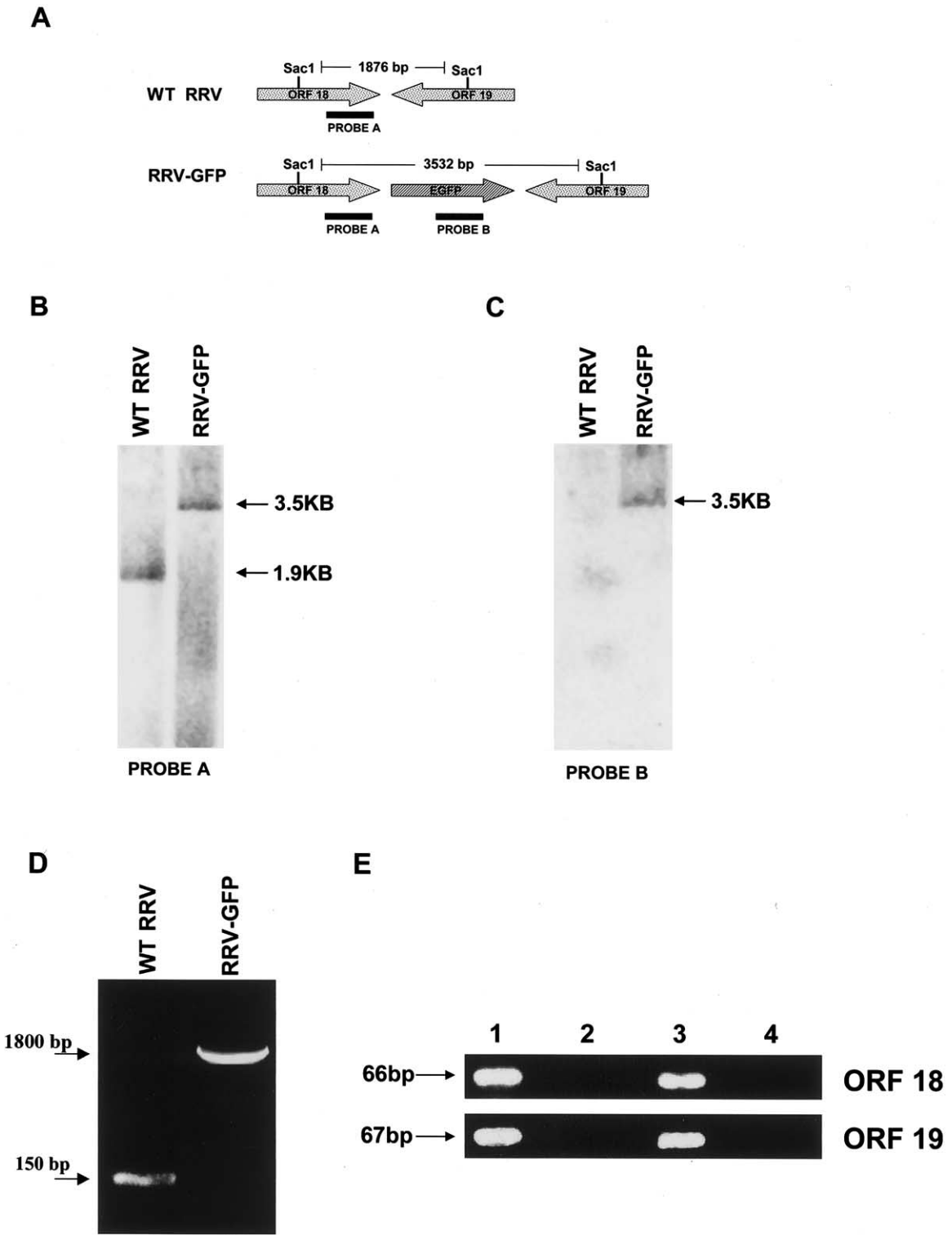

Fig. 3. Integrity and purity of the RRV-GFP recombinant. (A) Schematic representation of the *Sac*1 digestion of the RRV ORF 18/19 junction. Probe A was generated from digestion of a plasmid encoding RRV ORF 18, and probe B was generated from pEGFP-N1. (B) Southern hybridization performed with probe A, detected a 3.5-kb fragment from RRV-GFP and a 1.9-kb fragment from the parental strain. (C) An identical Southern blot as shown in (B) that has been hybridized with probe B containing the GFP gene. The same 3.5-kb fragment is apparent, and no other bands are present, confirming that the GFP cassette has only inserted into the ORF 18/19 junction. (D) PCR-amplification was performed using the wt RRV and RRV-GFP recombinant virus DNA with two different sets of primers in ORFs 18 and 19 that flank the insertion site. The arrows highlight the 1800 and 150 bp PCR-amplification products obtained from RRV-GFP and wt RRV viral DNA, respectively. (E) RT-PCR analysis of ORF18 and 19 gene expression in both recombinant (RRV-GFP) and parental virus (wt RRV). Lanes 1 and 2 represent the parental wt RRV virus, and lanes 3 and 4 represent the RRV-GFP virus. Lanes 2 and 4 represent samples in which no reverse transcriptase was added to the RT-PCR reaction.

ical applications (Dittmer et al., 1999; Fakhari and Dittmer, 2002; Gautheret-Dejean et al., 2002; Greenlee et al., 2002; Kimura et al., 2002; Lo et al., 2000; Pevenstein et al., 1999; Sanchez and Storch, 2002; White and Campbell, 2000).

In our assay, the target molecule for determining copy number in the RRV genome was the Orf50 gene. We chose this site for amplification because the Orf50 (Rta) homolog in other γ-herpesviruses has been shown to be one of the most essential lytic genes and the only protein necessary for reactivation from the latent state (Sun et al., 1998). For this reason, all functional copies of the RRV genome would have to contain a copy of the Orf50 gene. The real-time PCR primers and the probe were designed using the ABI Primer Express software program to ensure maximum amplification efficiency. An 81-base-pair amplicon was chosen as per the software recommendations, and we chose to use FAM as a reporter dye and TAMRA as a quencher dye in our dual-labeled probe.

A number of real-time PCR assays previously published report the use of uracil-*N*-glycosylase (UNG) as an additive to protect against carry-over contamination, whereby previously amplified product serves as a template for synthesis. All of our PCR reactions were carried out in a separate facility from where reactions were assembled, and a different designated individual removed the amplified samples from the machine and discarded them immediately. This careful procedure eliminated the risk of carry-over contamination because amplified product was never allowed back into the laboratory and made the use of UNG unnecessary for our purposes. Duplicate reactions containing either water or UNG were run and no difference was seen between their amplification profiles confirming this assumption (data not shown). As a further control for the accuracy of the real-time PCR assay, a rox dye included in the master mix was used to normalize samples for pipetting error.

The limit of detection for the RRV real-time PCR assay was near 10–50 copies per reaction, although the most accurate detection was in the range of 100 to 1 million template copies per reaction. For the set of reactions run in this article, the slope of the standard curve was −3.32 and the r^2 value was 0.992, and this was reproducible in all the experiments. PCR amplification efficiency, *k*, was calculated as a measure of exponential amplification (*E*), where $E = [10(-1/\text{slope})] - 1$ and $k = 1 + E$. Thus, the amplification efficiency is 1.995, which is close to the ideal amplification efficiency of $k = 2$ (Fakhari and Dittmer, 2002).

RRV one-step growth curve

To assess the functionality of our quantitative techniques and compare their results, we performed a one-step growth curve, which is the canonical assay for viral growth. Equivalent plaque forming units for both RRV H26-95, the wild-type strain, and RRV-GFP were used to infect RhFs at a multiplicity of infection of 5. At 24-h intervals after infection, cell-free supernatants were harvested and analyzed for viral titer by both plaque assay and real-time PCR. The results (Figs. 4A and B) show that RRV-GFP has nearly identical growth kinetics as wild-type RRV by both assays. The eclipse or lag phase for RRV seems to last at least 24 h but not more than 48 h. The single cycle of RRV replication is around 120 to 144 h, as no significantly greater amount of PFU/ml could be recovered after this time. Since we used equivalent plaque forming units for both RRV and RRV-GFP to infect RhFs, Fig. 4B shows a slight difference between the growth curves of RRV-GFP and wild-type virus in the real-time PCR data due to a larger amount of free unpackaged viral DNA in the RRV-GFP virus stock compared to the RRV.

Because the real-time PCR assay is a genome-counting assay, we are able to count viral DNA replication inside cells prior to viral egress. This is an advantage over the plaque assay, which counts functional viral particles that have exited the cell. Fig. 4C shows the intracellular viral DNA concentration during the growth curves for the two viruses. This type of analysis could prove to be very useful when studying recombinant viruses with DNA replication defects in future experiments. The RRV-GFP intracellular viral genome curve is slightly above that of wild-type RRV at early time points postinfection.

Sensitivity of RRV to replication inhibitors

To further show the utility of our assays for quantitation of viral titers, the recombinant RRV-GFP virus was tested for replication in the presence of a panel of compounds (Figs. 5A and B). The recombinant virus was used so that any results obtained by plaque assay and real-time PCR concerning the relative effect of the compounds could be correlated with the intensity of GFP expression as seen under the microscope during the course of the infection. The effect of two thymidine kinase (TK) directed antiviral compounds, acyclovir (ACV) and ganciclovir (GCV), as well as the herpesviral DNA polymerase inhibitor phosphonoacetic acid (PAA), were tested at various concentrations to see if each could effectively inhibit RRV replication up to 120 h postinfection. Also included was cyclohexamide, a general protein synthesis inhibitor, as a control.

It was concluded by the use of both quantitative assays that ACV was ineffective at reducing RRV replication at all concentrations tested. However, Kedes and Ganem (1997) have previously shown that there is a very slight inhibition of KSHV viral replication by acyclovir at high concentrations of the drug. GCV reduced RRV titer by 1 log when used at 100 μM, and by 2 logs when used at 500 μM. GCV at 1 mM completely abolished RRV replication, as did PAA at all concentrations as well as the positive control CHX at 0.5 μg/ml. The pattern of viral replication inhibition is consistent across the two assays, while the actual number of genomes versus plaque forming units differs, just as in the one-step growth curve. Although approximately 10 million RRV genomes per milliliter present in the samples we

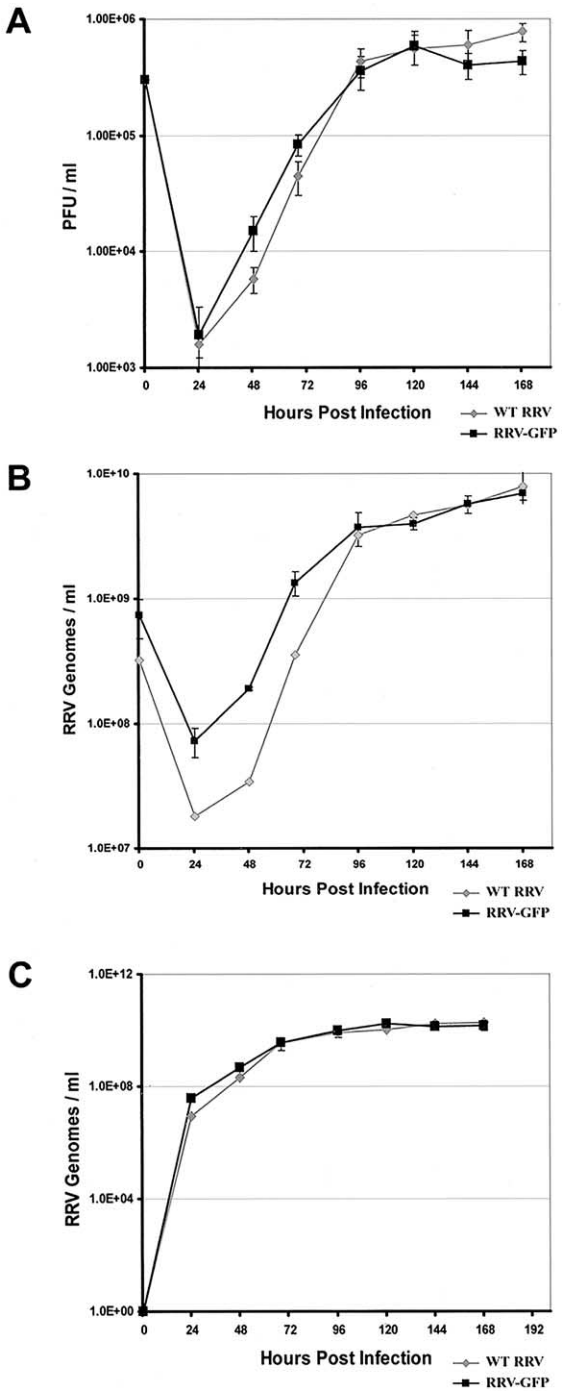

Fig. 4. RRV one-step growth curves. (A) Equivalent numbers of rhesus fibroblast cells were infected with either WT RRV H26-95 (gray diamonds) or RRV-GFP (black squares) at an m.o.i. of 5 and cell-free supernatants were harvested at indicated points postinfection and quantitated by plaque assay. (B) The same samples as in (A) were quantitated using the real-time PCR assay for RRV. (C) Intracellular virus concentration at indicated times after infection was quantitated by real-time PCR. Media were removed and cells were collected by trypsinization. Cells were lysed and DNA was extracted as described in Materials and methods.

report have no viral replication, it should be noted that this is the same copy number as was counted at 24 h postinfection during the one-step growth curve. Combined with the absence of plaques for these samples, we interpret this to mean that 10^7 is the approximate number of copies of the RRV genome that remains associated with the cells and the well itself after removal of the inoculum. Thus, these data points represent the complete inhibition of viral replication.

Comparing viral genomes to plaque forming units

By applying these two analyses to the same set of experiment samples, we can also compare the number of viral genomes per plaque forming unit. Table 1 shows the typical result for the ratio of genome copies per plaque at 48, 96, and 144 h postinfection, which ranges from around 1000 to 10,000. This ratio is slightly higher for the recombinant GFP-expressing virus and could possibly be due to the fact that when GFP is expressed at high levels it can become toxic to cells. This presents a possible scenario whereby cells undergoing viral replication begin to lyse because of the high expression levels of GFP, rather than viral egress, releasing large amounts of free viral DNA into the media without production of virus. Also listed in Table 1 are the ratios of PFU per genome copies.

Discussion

In this article, we present two new viral quantitation assays for rhesus monkey rhadinovirus, a useful animal model system to study KSHV and γ herpesvirus replication. We have compared the functionality of these assays to assess the replication kinetics of RRV and a recombinant RRV-GFP virus. We have thoroughly documented the purity and integrity of the RRV-GFP recombinant virus. We have also demonstrated that we have not disrupted transcription from the open reading frames flanking the site of insertion of the GFP cassette when creating the RRV-GFP recombinant virus. We have shown by two different quantitative assays that the wt RRV and RRV-GFP viruses display comparable replication kinetics. Further, we have subjected the virus to replication inhibitors in an attempt to utilize these assays to determine sensitivity of RRV to antiviral compounds.

According to one-step growth curves performed at an m.o.i. of 5, the amount of time it takes to complete a single replication cycle for RRV is approximately 120 to 144 h. The maximum titer achieved is approaching 1 million plaque forming units per milliliter for both the wild-type and the recombinant viruses. However, the number of viral genomes per milliliter of culture supernatant is around 10 billion. This observation could occur for a number of reasons, including the lysis of cells still undergoing viral DNA replication releasing unpackaged viral DNA prematurely. One way to circumvent this discrepancy in quantitation is to treat cell-free supernatants with DNAse to degrade free viral DNA. While this would rule out any difference due to free viral DNA, it would not take into account packaged repli-

cation-incompetent DNA. Because in these set of experiments we were only interested in observing the overall pattern of RRV replication, this step to rid samples of free viral DNA was omitted.

It has been previously reported that acyclovir is not an effective antiviral compound for KSHV by a majority of investigators (Neyts and De Clercq, 1997, and Kedes and Ganem, 1997, no. 2451). However, it moderately affects KSHV replication when used at very high concentrations (Medveczky et al., 1997), and one group reports ACV inhibits glycoprotein K8.1 expression, albeit not as well as PAA (Zoeteweij et al., 1999). In agreement with these data, our findings here report that RRV is unaffected by acyclovir at concentrations up to 1 mM. In contrast, studies in MHV-68 (Neyts and De Clercq, 1998) and EBV (Littler and Arrand, 1988; Moore et al., 2001) have shown that acyclovir is fairly effective at inhibiting replication, suggesting this insensitivity to acyclovir by RRV and KSHV is not a shared property of the TK gene of γ-herpesviruses in general.

Ganciclovir has been shown to be highly effective in inhibiting KSHV replication at low concentrations (Cannon et al., 1999; Dittmer et al., 1999; Kedes and Ganem, 1997; Neyts and De Clercq, 1997). However, one conflicting report suggests that the TK gene of KSHV is incapable of phosphorylating ganciclovir (Gustafson et al., 2000). With regard to ganciclovir, RRV is not significantly inhibited at 10 μM concentration, but suffers successive 1 log reductions at 100 and 500 μM, respectively, and replication is completely abolished at a 1 mM concentration of ganciclovir. While the concentrations tested are much higher for RRV due to the completely lytic nature of our system, the general pattern is consistent with what has been shown for KSHV reactivation from BCBL-1 cells (Kedes and Ganem, 1997). Differing reports exist for the efficacy of ganciclovir on EBV, while some show it is very effective at killing EBV TK-expressing cells (Littler and Arrand, 1988; Moore et al., 2001; Rogers et al., 1996); others report that the EBV TK gene by itself cannot phosphorylate ganciclovir (Gustafson et al., 1998). MHV-68 showed a similar sensitivity to ganciclovir (Neyts and De Clercq, 1998), suggesting that this compound is an effective choice for inhibiting replication in all γ-herpesviruses (Neyts and De Clercq, 1998).

PAA and foscarnet are two herpesviral DNA polymerase inhibitors with the same mechanism of action. PAA was inhibitory at all concentrations tested for RRV. This finding is not surprising considering data from other herpesviruses, which shows that the DNA polymerase gene for these viruses is highly conserved. PAA and PFA have been shown to be highly effective inhibitors of KSHV reactivation in a number of reports (Kedes and Ganem, 1997; Lin and Ricciardi, 2000; Low et al., 1998; Medveczky et al., 1997; Zoeteweij et al., 1999).

While in all cases mentioned above, both quantitative assays were able to accurately measure the effectiveness of antiviral compounds, one aspect of the real-time PCR assay is its sensitivity to various PCR inhibitors. While most known PCR inhibitors are derived from in vivo fluid or tissue samples, the existing possibility that compounds used in vitro could inhibit a PCR reaction was best illustrated to us while performing the replication inhibition study. Polybrene, a polycationic lipid previously reported to increase the infectivity of a number of viruses (Andreadis and Palsson, 1997; Damico and Bates, 2000) including KSHV (Lagunoff et al., 2002), was included at four concentrations to test its effect on RRV infectivity. Unexpectedly, it was found that the samples containing polybrene at all concentrations failed to amplify during real-time PCR, despite the cleaning of the samples using DNA-binding columns. The Ct values reported for these samples were even lower than the no-template control reactions, and the effect was dose-dependent, which perhaps suggests that polybrene is a very strong inhibitor of some aspect of the PCR reaction. This could represent a failure to amplify target DNA, or an inhibition of fluorescent emission, among a number of possibilities. As a result, this finding precludes the use of the real-time PCR assay in any studies involving polybrene as a replication enhancer, until better purification methods are implemented.

Application of these assays to in vitro and in vivo studies will undoubtedly assist future studies in RRV. Deciding which assay to use will need to be dictated by the specific experiments being performed. For example, a recombinant RRV that is deleted for a gene necessary for the structure of the virion will not likely show any major DNA replication defect, and as such its replication kinetics will appear identical to wild-type RRV when measured by the real-time PCR assay. However, because this virus would not be able to form infectious particles, the plaque assay would be the best choice to highlight the replication defect. In contrast, the real-time PCR assay also has specific advantages when applying a forward genetic approach. In the case where an isolated mutant virus exhibits a slight replication defect when measured by the plaque assay, the real-time PCR technique would help to determine if this defect was occurring before or after the stage of viral DNA replication.

In summary, we have outlined the protocols for two new viral titration assays for the quantitation of RRV, which serves as an animal model system to study the KSHV viral lifecycle and pathogenesis. These methodologies lay the foundation for future studies involving RRV, and the study of γ-herpesvirus pathogenesis, in general. We have also demonstrated for the first time that we can construct a RRV-GFP recombinant virus using a traditional homologous recombination strategy. This virus will prove useful in studies of RRV in its natural host, the rhesus monkey.

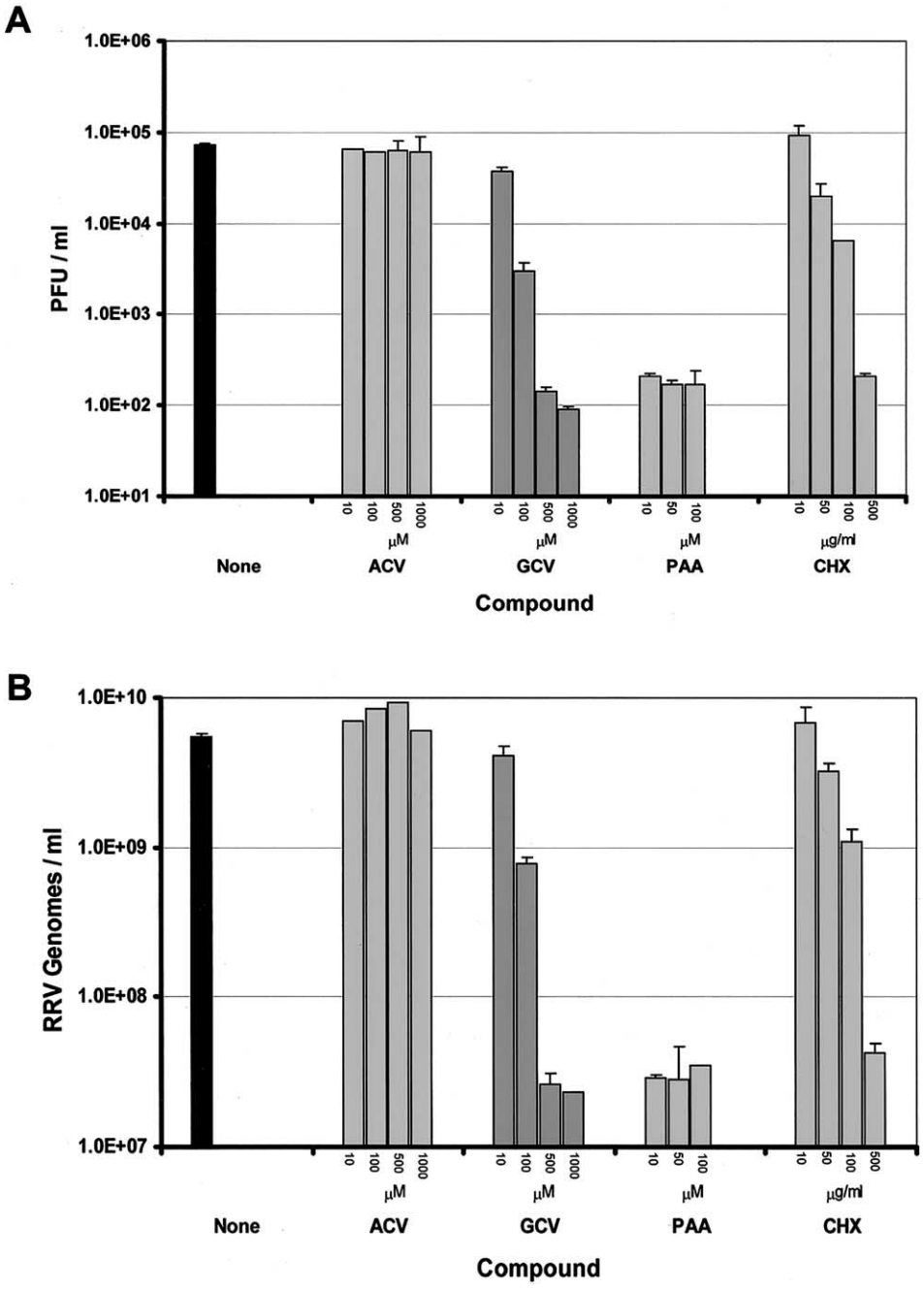

Fig. 5. Sensitivity of RRV to replication inhibitors. RRV-GFP was used at an m.o.i. of 5 to infect equal numbers of rhesus fibroblast cells for 120 h in the presence of various inhibitors of herpesviral replication at the concentrations shown: acyclovir (ACV), ganciclovir (GCV), phosphonoacetic acid (PAA), and as a control cyclohexamide (CHX). Viral titers were determined by plaque assay (as in A) or real-time PCR (as in B).

Materials and methods

Cell culture

Rhesus macaque skin fibroblasts were immortalized as previously described (DeWire, et al., 2002). Cells were maintained at 37°C and 5% CO_2 in Dulbecco's modified Eagle's medium-H (DMEM-H) with Gluta-max supplemented with 10% fetal bovine serum.

Virus and infections

RRV isolate H26-95 (Alexander et al., 1999) was used to infect rhesus fibroblasts at a multiplicity of infection (m.o.i.) of approximately 1 by standard protocols (Cann, 1999). Ganciclovir, acyclovir, cyclohexamide (Sigma C7698), and phosphonoacetic acid (Sigma P6909) were used at concentrations described in the figure legends. All compounds were added as a mixture in fresh media after 1 h of viral

Table 1
Comparison of viral genomes to plaque forming units

h.p.i.	PFU/ml	Genomes/ml	Ratio (Genomes/PFU)	Ratio (PFU/genome)
RRV H26-95				
48	5.83×10^3	3.4×10^7	5.9×10^3	0.00016
96	4.33×10^5	3.2×10^9	7.4×10^3	0.00014
144	6.0×10^5	5.6×10^9	9.4×10^3	0.00011
RRV-GFP				
48	1.50×10^4	1.9×10^8	1.3×10^4	0.00008
96	3.58×10^5	3.7×10^9	1.0×10^4	0.00009
144	4.0×10^5	5.7×10^9	1.4×10^4	0.00007

infection. At various time points after infection cell-free supernatants were harvested by centrifugation at 2000 rpm for 5 min. For intracellular viral assays, any cellular material pelleted from the above centrifugation was combined with infected cells harvested by trypsinization in 500 μl PBS.

Recombinant RRV-GFP virus

A 3051-bp region of RRV H26-95 spanning nucleotides 24788 to 27839 was PCR amplified with primers 5′-CGCCGCCTCGAGATGGCGGCTGTTCAGGGCCCT-3′ and 5′-CGCCGCCTGCAGCTACACTACGCTGTTATTGA-3′. This product was subsequently cloned into pSP72 (Promega) at *Xho*1 and *Pst*1 restriction sites to create pSP72-LFR. A 3862-bp region of RRV H26-95 spanning nucleotides 27847 to 31709 was PCR amplified with primers 5′-CGCCGCGGATCCTCACACTACCGACGTGGCGACC-3′ and 5′-CGCCGCGATATCTTAATTGGCTGCATTGCTTT-3′. This product was subsequently cloned into pSP72-LFR at *Bam*H1 and *Eco*RV restriction sites to create pSP72-LFR-RFR. The multiple cloning site from pEGFP-N1 (Clontech) was deleted by performing a *Bam*H1 and *Bgl*II double digest, and then re-ligating the resulting vector to form pEGFP-N1-ΔMCS. The EGFP expression cassette driven by the CMV IE promoter with the SV40 polyadenylation signal was PCR amplified from pEGFP-N1-ΔMCS with the I-Ceul and I-Scel tagged primers 5′-CGCCGCCTGCAGTAACTATAACGGTCCTAAGGTAGCGAGTAATCAATTACGGGGTCATTAGTTCATAGCCC-3′ and 5′-CGCCGCGGATCCTAGGGATAACAGGGTAATGGACAAACCACAACTAGAATGCAGTG-3′. The resulting PCR product was ligated into pSP72-LFR-RFR to form pSP72-LFR-GFP-RFR. This plasmid was then cotransfected with RRV-H26-95-purified viral DNA by electroporation into RhFs at 250 V and 500 μF. A single GFP-positive virus was isolated and purified by limiting dilution four times and by flow cytometry once.

Integrity of recombinant RRV genome

PCR primers corresponding to the ends of ORF18 and ORF19 were used in a PCR reaction with either RRV-H26-95 or RRV-GFP as a template. Primers were 5′-GATTTCGGCGTGGGATTTTGCGTCCGC-3′ and 5′-CGAGATAATGAAAAGCCAATTCGGAGT-3′. Expected product sizes were ~150 bp for RRV-H26-95 and ~1800 bp for RRV-GFP. The 1800 and 150 bp PCR products from the recombinant and wt viruses were subsequently sequenced to confirm the presence of the CMV-EGFP-pA cassette.

Southern hybridization

Virus was harvested from cell-free media from virus-infected cells by centrifugation at 15,000 rpm for 3 h. Virus pellet was resuspended in PBS and treated with proteinase K for 2 h at 56°C. Viral DNA was extracted by phenol-chloroform method and subsequently digested with *Sac*1. Digestions were electrophoresed through 1% low-melt agarose (NuSieve) 1× TBE and transferred to a nylon membrane (Hybond N+) by capillary action. Following UV cross-linking, membranes were prehybridized in QuikHyb solution at 65°C for 15 min. Probes were generated from RRV-ORF18 and GFP by random prime method using ^{32}P (Roche). Probes were denatured at 95°C for 3 min and added to prehybe solution. Hybridization was carried out for 16 h at 65°C. Probe solution was removed and membranes were washed twice for 15 min with 2× SSC 0.1% SDS at room temperature and once for 30 min at 60°C with 0.1× SSC 0.1% SDS. Membranes were exposed and read on a PhosphorImager Scanner (Molecular Dynamics).

RT-PCR of ORFs 18 and 19

Total RNA was extracted from RhF's infected with either RRV-H26-95 or RRV-GFP for 3 days using the RNA-Stat 60 protocol as previously described (DeWire et al., 2002). The poly A fraction was subsequently isolated using the OligoTex system (Qiagen) according to the manufacturer's protocol. Poly A RNA was then DNase1 treated by the RQ1 protocol (Promega), and RT-PCR was performed with the Superscript One-Step RT-PCR system (Invitrogen) as per manufacturer's protocol using equivalent micrograms of starting poly A RNA. Primers were designed by W. Vahrson (Bioinformatics Consulting & Software Development). Primers used for ORF 18 were 5′-GAACCAAAAGCTCACGTTCAG-3′ and 5′-GATGGGTGCGAGAGGATG-3′. Primers used for ORF 19 were 5′-CGCGTTCGTTGTCACAATAG-3′ and 5′-AGCCATTGGTTTTGGTTCAT-3′. Expected product sizes were 67 and 66 base pairs, respectively.

Quantitative real-time PCR

For each sample, 10 μg of salmon sperm carrier DNA was added to 200 μl of clarified supernatant from infected cells and was processed through the QiaAmp DNA Blood Mini Kit (Qiagen) as per the manufacturer's protocol. As a set of internal standards, the plasmid pcDNA3-RRVOrf50 (DeWire et al., 2002) was serially diluted to known concentrations in the range of 10^1 to 10^7 plasmid molecules per microliter with the total concentration of DNA in each adjusted to 50 μg/ml with salmon sperm DNA. PCR reactions were prepared using the Quantitect probe-PCR kit (Qiagen) in 20 μl volumes. Primers for amplification of an 81-bp amplicon internal to the Orf50 sequence were 5′-GTGGAAAGCGGTGTCACAGA-3′ and 5′-TGCGGCG-GCCAAAAT-3′ and the probe was 5′ FAM-TTCACCAC-CAGGCACAGACGCC-TAMRA-3′. Reactions were run in 384-well format in an ABI Prism 7900HT with the following conditions: 95°C for 15 min, followed by 95°C for 15 s, 60°C for 1 min repeated for 40 cycles. Cts were determined as the first cycle where fluorescence was 10 times background. PCR amplification efficiency, *k*, was calculated as a measure of exponential amplification (*E*), where $E = [10(-1/\text{slope})] - 1$ and $k = 1 + E$. The slope was calculated to be -3.32. The amplification efficiency was calculated to be 1.995, which is close to the ideal amplification efficiency of $k = 2$ (Fakhari and Dittmer, 2002).

Plaque assays

Monolayers of RhFs in 12-well plates were achieved by plating 2×10^5 cells per well 2 days before starting the assay. Dilutions of virus-infected cell supernatants were made in DMEM-H supplemented with 2% bovine calf serum (BCS). Each sample dilution was performed in triplicate. Two hundred microliters of each dilution was placed in each well of 12-well dishes and incubated at 37°C for 1 h with redistribution of inoculum every 15 min. Inoculum was aspirated and an overlay media was added to each well consisting of (per well): 1 ml 2×DMEM, 1 ml 1.5% methyl-cellulose (Sigma M0512), and 40 μl BCS (2%). Plaque assays were then incubated 7 days at 37°C and 5% CO_2. Overlay media was then aspirated and staining solution (0.8% crystal violet (Sigma C3886), 50% ethanol) was added to each well and incubated 10 min. Plaques were counted under ×10 magnification.

Acknowledgments

We are grateful to S. Bachenheimer for invaluable advice regarding plaque assays and providing acyclovir, S. Kenney for providing ganciclovir, and Q.Yang for assistance with real-time PCR. We thank W. Vahrson for the design of the RRV RT-PCR primers, R. Desrosiers for RRV strain H26-95, and D. Dittmer for manuscript reading. We also thank members of the Damania lab for informative discussions. S. DeWire is supported, in part, by NIH training Grant 5T32GM07092-26. This work was supported in part by grants from the V Foundation, UNC-CFAR, American Heart Association, and NIH/NCI Grant CA096500.

References

Alexander, L., Denenkamp, L., Knapp, A., Auerbach, M., Czajak, S., Damania, B., Desrosiers, R.C., 1999. The primary sequence of rhesus rhadinovirus isolate 26-95: sequence similarities to Kaposi's sarcoma-associated herpesvirus and rhesus rhadinovirus isolate 17577. J. Virol. 74 (7), 3388–3398.

Andreadis, S., Palsson, B.O., 1997. Coupled effects of polybrene and calf serum on the efficiency of retroviral transduction and the stability of retroviral vectors. Hum. Gene Ther. 8 (3), 285–291.

Bosch, M.L., Harper, E., Schmidt, A., Strand, K.B., Thormahlen, S., Thouless, M.E., Wang, Y., 1999. Activation in vivo of retroperitoneal fibromatosis-associated herpesvirus, a simian homologue of human herpesvirus-8. J. Gen. Virol. 80 (Pt 2), 467–475.

Cann, A.J., (1999). DNA viruses: a practical approach. Practical Approach Series 214.

Cannon, J.S., Hamzeh, F., Moore, S., Nicholas, J., Ambinder, R.F., 1999. Human herpesvirus 8-encoded thymidine kinase and phosphotransferase homologues confer sensitivity to ganciclovir. J. Virol. 73 (6), 4786–4793.

Cesarman, E., Chang, Y., Moore, P.S., Said, J.W., Knowles, D.M., 1995. Kaposi's sarcoma-associated herpesvirus-like DNA sequences in AIDS-related body-cavity-based lymphomas. N. Engl. J. Med. 332 (18), 1186–1191.

Chan, S.R., Bloomer, C., Chandran, B., 1998. Identification and characterization of human herpesvirus-8 lytic cycle-associated ORF 59 protein and the encoding cDNA by monoclonal antibody. Virology 240 (1), 118–126.

Chang, Y., Cesarman, E., Pessin, M.S., Lee, F., Culpepper, J., Knowles, D.M., Moore, P.S., 1994. Identification of herpesvirus-like DNA sequences in AIDS-associated Kaposi's sarcoma. Science 266 (5192), 1865–1869.

Damania, B., DeMaria, M., Jung, J.U., Desrosiers, R.C., 2000. Activation of lymphocyte signaling by the R1 protein of rhesus monkey rhadinovirus. J. Virol. 74 (6), 2721–2730.

Damania, B., Li, M., Choi, J.K., Alexander, L., Jung, J.U., Desrosiers, R.C., 1999. Identification of the R1 oncogene and its protein product from the rhadinovirus of rhesus monkeys. J. Virol. 73 (6), 5123–5131.

Damico, R., Bates, P., 2000. Soluble receptor-induced retroviral infection of receptor-deficient cells. J. Virol. 74 (14), 6469–6475.

Desrosiers, R.C., Sasseville, V.G., Czajak, S.C., Zhang, X., Mansfield, K.G., Kaur, A., Johnson, R.P., Lackner, A.A., Jung, J.U., 1997. A herpesvirus of rhesus monkeys related to the human Kaposi's sarcoma-associated herpesvirus . J. Virol. 71 (12), 9674–9769.

DeWire, S.M., McVoy, M.A., Damania, B., 2002. Kinetics of expression of rhesus monkey rhadinovirus (RRV) and identification and characterization of a polycistronic transcript encoding the RRV Orf50/Rta, RRV R8, and R8.1 Genes. J. Virol. 76 (19), 9819–9831.

Dezube, B.J., Zambela, M., Sage, D.R., Wang, J.F., Fingeroth, J.D., 2002. Characterization of Kaposi sarcoma-associated herpesvirus/human herpesvirus-8 infection of human vascular endothelial cells: early events. Blood 100 (3), 888–896.

Dittmer, D., Stoddart, C., Renne, R., Linquist-Stepps, V., Moreno, M.E., Bare, C., McCune, J.M., Ganem, D., 1999. Experimental transmission of Kaposi's sarcoma-associated herpesvirus (KSHV/HHV-8) to SCID-hu Thy/Liv mice. J. Exp. Med. 190 (12), 1857–1868.

Fakhari, F.D., Dittmer, D.P., 2002. Charting latency transcripts in Kaposi's sarcoma-associated herpesvirus by whole-genome real-time quantitative PCR. J. Virol. 76 (12), 6213–6223.

Ganem, D., 1998. Human herpesvirus 8 and its role in the genesis of Kaposi's sarcoma. Curr. Clin. Top. Infect. Dis. 18, 237–251.

Garabedian, G.A., Scott, L.V., 1967. Plaque assay for herpes simplex virus in L-929 (Earle) mouse fibroblasts. Proc. Soc. Exp. Biol. Med. 126 (2), 568–571.

Gautheret-Dejean, A., Manichanh, C., Thien-Ah-Koon, F., Fillet, A.M., Mangeney, N., Vidaud, M., Dhedin, N., Vernant, J.P., Agut, H., 2002. Development of a real-time polymerase chain reaction assay for the diagnosis of human herpesvirus-6 infection and application to bone marrow transplant patients. J. Virol. Methods 100 (1–2), 27–35.

Gerna, G., Chambers, R.W., 1976. Varicella-zoster plaque assay and plaque reduction neutralization test by the immunoperoxidase technique. J. Clin. Microbiol. 4 (5), 437–442.

Gessain, A., Sudaka, A., Briere, J., Fouchard, N., Nicola, M.A., Rio, B., Arborio, M., Troussard, X., Audouin, J., Diebold, J., 1996. Kaposi sarcoma-associated herpes-like virus (human herpesvirus type 8) DNA sequences in multicentric Castleman's disease: is there any relevant association in non-human immunodeficiency virus-infected patients? Blood 87 (1), 414–416.

Greenlee, D.J., Fan, H., Lawless, K., Harrison, C.R., Gulley, M.L., 2002. Quantitation of CMV by real-time PCR in transfusable RBC units. Transfusion 42 (4), 403–408.

Gustafson, E.A., Chillemi, A.C., Sage, D.R., and Fingeroth, J.D., 1998. The Epstein-Barr virus thymidine kinase does not phosphorylate ganciclovir or acyclovir and demonstrates a narrow substrate specificity compared to the herpes simplex virus type 1 thymidine kinase. Antimicrob. Agents Chemother. 42 (11), 2923–2931.

Gustafson, E.A., Schinazi, R.F., Fingeroth, J.D., 2000. Human herpesvirus 8 open reading frame 21 is a thymidine and thymidylate kinase of narrow substrate specificity that efficiently phosphorylates zidovudine but not ganciclovir. J. Virol. 74 (2), 684–692.

Heid, C.A., Stevens, J., Livak, K.J., Williams, P.M., 1996. Real time quantitative PCR. Genome Res. 6 (10), 986–994.

Jung, J.U., Choi, J.K., Ensser, A., Biesinger, B., 1999. Herpesvirus saimiri as a model for gammaherpesvirus oncogenesis. Semin. Cancer Biol. 9 (3), 231–239.

Kaleeba, J.A., Bergquam, E.P., Wong, S.W., 1999. A rhesus macaque rhadinovirus related to Kaposi's sarcoma-associated herpesvirus/human herpesvirus 8 encodes a functional homologue of interleukin-6. J. Virol. 73 (7), 6177–6181.

Kedes, D.H., Ganem, D., 1997. Sensitivity of Kaposi's sarcoma-associated herpesvirus replication to antiviral drugs. Implications for potential therapy. J. Clin. Invest. 99 (9), 2082–2086.

Kedes, D.H., Operskalski, E., Busch, M., Kohn, R., Flood, J., Ganem, D., 1996. The seroepidemiology of human herpesvirus 8 (Kaposi's sarcoma-associated herpesvirus): distribution of infection in KS risk groups and evidence for sexual transmission. Nat. Med. 2 (8), 918–924.

Kimura, H., Ito, Y., Futamura, M., Ando, Y., Yabuta, Y., Hoshino, Y., Nishiyama, Y., Morishima, T., 2002. Quantitation of viral load in neonatal herpes simplex virus infection and comparison between type 1 and type 2. J. Med. Virol. 67 (3), 349–353.

Lagunoff, M., Bechtel, J., Venetsanakos, E., Roy, A.M., Abbey, N., Herndier, B., McMahon, M., Ganem, D., 2002. De novo infection and serial transmission of Kaposi's sarcoma-associated herpesvirus in cultured endothelial cells. J. Virol. 76 (5), 2440–2448.

Lin, K., Ricciardi, R.P., 2000. A rapid plate assay for the screening of inhibitors against herpesvirus DNA polymerases and processivity factors. J. Virol. Methods 88 (2), 219–225.

Lin, S.F., Robinson, D.R., Oh, J., Jung, J.U., Luciw, P.A., Kung, H.J., 2002. Identification of the bZIP and Rta homologues in the genome of rhesus monkey rhadinovirus. Virology 298 (2), 181–188.

Littler, E., Arrand, J.R., 1988. Characterization of the Epstein–Barr virus-encoded thymidine kinase expressed in heterologous eucaryotic and procaryotic systems. J. Virol. 62 (10), 3892–3895.

Lo, Y.M., Chan, A.T., Chan, L.Y., Leung, S.F., Lam, C.W., Huang, D.P., Johnson, P.J., 2000. Molecular prognostication of nasopharyngeal carcinoma by quantitative analysis of circulating Epstein–Barr virus DNA. Cancer Res. 60 (24), 6878–6881.

Low, P., Neipel, F., Rascu, A., Steininger, H., Manger, B., Fleckenstein, B., Kalden, J.R., Harrer, T., 1998. Suppression of HHV-8 viremia by foscarnet in an HIV-infected patient with Kaposi's sarcoma and HHV-8 associated hemophagocytic syndrome. Eur. J. Med. Res. 3 (10), 461–464.

Medveczky, M.M., Horvath, E., Lund, T., Medveczky, P.G., 1997. In vitro antiviral drug sensitivity of the Kaposi's sarcoma-associated herpesvirus. AIDS 11 (11), 1327–1332.

Miller, G., Heston, L., Grogan, E., Gradoville, L., Rigsby, M., Sun, R., Shedd, D., Kushnaryov, V.M., Grossberg, S., Chang, Y., 1997. Selective switch between latency and lytic replication of Kaposi's sarcoma herpesvirus and Epstein–Barr virus in dually infected body cavity lymphoma cells. J. Virol. 71 (1), 314–324.

Miller, G., Rigsby, M.O., Heston, L., Grogan, E., Sun, R., Metroka, C., Levy, J.A., Gao, S.J., Chang, Y., Moore, P., 1996. Antibodies to butyrate-inducible antigens of Kaposi's sarcoma-associated herpesvirus in patients with HIV-1 infection. N. Engl. J. Med. 334 (20), 1292–1297.

Moore, P.S., Chang, Y., 1995. Detection of herpesvirus-like DNA sequences in Kaposi's sarcoma in patients with and without HIV infection. N. Engl. J. Med. 332 (18), 1181–1185.

Moore, S.M., Cannon, J.S., Tanhehco, Y.C., Hamzeh, F.M., Ambinder, R.F., 2001. Induction of Epstein–Barr virus kinases to sensitize tumor cells to nucleoside analogues. Antimicrob. Agents Chemother. 45 (7), 2082–2091.

Neyts, J., De Clercq, E., 1997. Antiviral drug susceptibility of human herpesvirus 8. Antimicrob. Agents Chemother. 41 (12), 2754–2756.

Neyts, J., De Clercq, E., 1998. In vitro and in vivo inhibition of murine gamma herpesvirus 68 replication by selected antiviral agents. Antimicrob. Agents Chemother. 42 (1), 170–172.

Pevenstein, S.R., Williams, R.K., McChesney, D., Mont, E.K., Smialek, J.E., Straus, S.E., 1999. Quantitation of latent varicella-zoster virus and herpes simplex virus genomes in human trigeminal ganglia. J. Virol. 73 (12), 10514–10518.

Renne, R., Blackbourn, D., Whitby, D., Levy, J., Ganem, D., 1998. Limited transmission of Kaposi's sarcoma-associated herpesvirus in cultured cells. J. Virol. 72 (6), 5182–5188.

Renne, R., Zhong, W., Herndier, B., McGrath, M., Abbey, N., Kedes, D., Ganem, D., 1996. Lytic growth of Kaposi's sarcoma-associated herpesvirus (human herpesvirus 8) in culture. Nat. Med. 2 (3), 342–346.

Rogers, R.P., Ge, J.Q., Holley-Guthrie, E., Hoganson, D.K., Comstock, K.E., Olsen, J.C., Kenney, S., 1996. Killing Epstein–Barr virus-positive B lymphocytes by gene therapy: comparing the efficacy of cytosine deaminase and herpes simplex virus thymidine kinase. Hum. Gene Ther. 7 (18), 2235–2245.

Roizman, B., Jenkins, F.J., 1985. Genetic engineering of novel genomes of large DNA viruses. Science 229 (4719), 1208–1214.

Rose, T.M., Strand, K.B., Schultz, E.R., Schaefer, G., Rankin Jr., G.W., Thouless, M.E., Tsai, C.C., Bosch, M.L., 1997. Identification of two homologs of the Kaposi's sarcoma-associated herpesvirus (human herpesvirus 8) in retroperitoneal fibromatosis of different macaque species. J. Virol. 71 (5), 4138–4144.

Sakurada, S., Katano, H., Sata, T., Ohkuni, H., Watanabe, T., Mori, S., 2001. Effective human herpesvirus 8 infection of human umbilical vein endothelial cells by cell-mediated transmission. J. Virol. 75 (16), 7717–7722.

Sanchez, J.L., Storch, G.A., 2002. Multiplex, quantitative, real-time PCR assay for cytomegalovirus and human DNA. J. Clin. Microbiol. 40 (7), 2381–2386.

Schultz, E.R., Rankin Jr., G.W., Blanc, M.P., Raden, B.W., Tsai, C.C., Rose, T.M., 2000. Characterization of two divergent lineages of macaque rhadinoviruses related to Kaposi's sarcoma-associated herpesvirus. J Virol 74 (10), 4919–4928.

Searles, R.P., Bergquam, E.P., Axthelm, M.K., Wong, S.W., 1999. Sequence and genomic analysis of a rhesus macaque rhadinovirus with similarity to Kaposi's sarcoma-associated herpesvirus/human herpesvirus 8. J. Virol. 73 (4), 3040–3053.

Simas, J.P., Efstathiou, S., 1998. Murine gammaherpesvirus 68: a model for the study of gammaherpesvirus pathogenesis. Trends Microbiol. 6 (7), 276–282.

Soulier, J., Grollet, L., Oksenhendler, E., Cacoub, P., Cazals-Hatem, D., Babinet, P., d'Agay, M.F., Clauvel, J.P., Raphael, M., Degos, L., et al., 1995. Kaposi's sarcoma-associated herpesvirus-like DNA sequences in multicentric Castleman's disease. Blood 86 (4), 1276–1280.

Strand, K., Harper, E., Thormahlen, S., Thouless, M.E., Tsai, C., Rose, T., Bosch, M.L., 2000. Two distinct lineages of macaque gamma herpesviruses related to the Kaposi's sarcoma associated herpesvirus. J. Clin. Virol. 16 (3), 253–269.

Sun, R., Lin, S.F., Gradoville, L., Yuan, Y., Zhu, F., Miller, G., 1998. A viral gene that activates lytic cycle expression of Kaposi's sarcoma- associated herpesvirus. Proc. Natl. Acad. Sci. USA 95 (18), 10866–10871.

Wentworth, B.B., French, L., 1969. Plaque assay of Herpesvirus hominis on human embryonic fibroblasts. Proc. Soc. Exp. Biol. Med. 131 (2), 588–592.

Wentworth, B.B., French, L., 1970. Plaque assay of cytomegalovirus strains of human origin. Proc. Soc. Exp. Biol. Med. 135 (2), 253–258.

White, I.E., Campbell, T.B., 2000. Quantitation of cell-free and cell-associated Kaposi's sarcoma-associated herpesvirus DNA by real-time PCR. J. Clin. Microbiol. 38 (5), 1992–1995.

Yazaki, S., Taniguchi, S., Yoshino, K., 1966. Improvement of the plaque assay of herpes simplex virus in HeLa cells. Jpn. J. Microbiol. 10 (3), 133–139.

Zhou, F.C., Zhang, Y.J., Deng, J.H., Wang, X.P., Pan, H.Y., Hettler, E., Gao, S.J., 2002. Efficient infection by a recombinant Kaposi's sarcoma-associated herpesvirus cloned in a bacterial artificial chromosome: application for genetic analysis. J. Virol. 76 (12), 6185–6196.

Zoeteweij, J.P., Eyes, S.T., Orenstein, J.M., Kawamura, T., Wu, L., Chandran, B., Forghani, B., Blauvelt, A., 1999. Identification and rapid quantification of early- and late-lytic human herpesvirus 8 infection in single cells by flow cytometric analysis: characterization of antiherpesvirus agents. J. Virol. 73 (7), 5894–5902.